Fiber Element Model of Sandwich Panels with Soft Cores and Composite Skins in Bending Considering Large Shear…

Article *in* Journal of Engineering Mechanics · January 2016

DOI: 10.1061/(ASCE)EM.1943-7889.0001062

3 authors:

Amir Fam
Queen's University

Tarek Sharaf
Port Said University

Pedram Sadeghian
Dalhousie University

Fiber Element Model of Sandwich Panels with Soft Cores and Composite Skins in Bending Considering Large Shear Deformations and Localized Skin Wrinkling

Amir Fam, MASCE [1], Tarek Sharaf [2], Pedram Sadeghian [3]

Abstract

This paper studies the flexural performance of sandwich panels composed of a soft polyurethane foam core and glass fibre-reinforced polymer (GFRP) skins. A robust analytical model is developed to predict the full load-deflection and strain responses of the panel. It is based on equilibrium and strain compatibility and accounts for the excessive shear deformation and material nonlinearity of the core. It also accounts for geometric nonlinearity in the form of localized deflection of the loaded skin using the principals of beam-on-elastic foundation and the change in core thickness due to its softness. The model incorporates various failure criteria, namely core shear failure, core flexural tension or compression failure, compression skin crushing or wrinkling, or tensile rupture of skin. The model has the advantage of being able to isolate quantitatevely the individual contributions of flexure, shear, and localized skin deformations, to overall deflection. A parametric study is performed to examine the effects of core density and skin thickness on panel behavior. It is shown that as the core density increases from 32 to 192 kg/m^3, the contribution of shear to overall deflection reduces from about 90 to 10 percent. It also appears that the optimal core density of the sandwich panels is within 96 to 128 kg/m^3, which represents the lowest density necessary to achieve the highest ultimate strength and stiffness.

Keywords: Sandwich panel; Model; FRP skin; Polyurethane core; Flexure; Shear; Wrinkling.

[1] Donald and Sarah Munro Chair Professor in Engineering and Applied Science, Department of Civil Engineering, Queen's University, Kingston, ON, K7L 3N6 Canada. E-mail: fam@civil.queensu.ca
[2] Former Doctoral Student, Department of Civil Engineering, Queen's University, Kingston, ON, K7L 3N6 Canada.
[3] Former Post-doctoral Fellow, Department of Civil Engineering, Queen's University, Kingston, ON, K7L 3N6 Canada.

INTRODUCTION

Civil engineering applications, particularly cladding of buildings, decking, and roofing can benefit greatly from sandwich panel systems. The skins, which resist flexure, are generally made of metals or composite materials such glass fibre-reinforced polymer (GFRP). The core generally carries the shear and provides the necessary spacing of skins. One of the commonly used core materials is polyurethane foam due to its low density and thermal insulation characteristics. Some of the earliest applications of sandwich panels in the 20th century were in aircraft industry (Allen, 1969). This was followed by expansion into the aerospace, automotive, and marine industries. Early on, sandwich panels fabricated from metallic cores were assumed to be incompressible (i.e. with negligible through-thickness deformation) and also negligible contribution to the flexural stiffness (Holt and Webber, 1982 and Pearce, 1973). Others made the assumption that sandwich panels with a foam core act like an ordinary beam with equivalent sectional properties (Ogorkiewicz and Sayigh, 1973). Sandwich panels with incompressible cores were analyzed using the "shear deformable approach" (Kant and Mallikarjuna, 1989; Kant and Patil, 1991; Senthilnathan et al., 1988; and Chandrashekhara and Krishnamurthy, 1990). However, the assumption of incompressible core was not accurate for flexible cores. Frostig and Baruch (1990) recognized this, particularly the localized compressibility in the vicinity applied loads. Closed-form equations for predicting deflection, normal stresses in skins, and core shear stresses were developed earlier by Allen (1969), neglecting core flexibility, while Frostig and Baruch (1990) developed the governing differential equations for these engineering quantities based on superposition approach, accounting for core flexibility, but without giving closed-form equations. A high-order bending theory based on virtual work was later developed by Frostig et al. (1992), as an alternative to superposition, to generate the governing deferential equation to predict the bending behaviour of a sandwich beam with flexible core. The theory was later improved by Frostig (1993) to consider the effect of stress concentration under different types of loads in various regions of the panel. Frostig et al. (2005) presented the governing equations of a sandwich panel, which has a transversely flexible core with negligible flexural rigidity, including large displacements. The study took into account the nonlinearity, not only in the core, but also in the skins. Shen et al. (2004) used the high-order sandwich panel theory to predict the bending behaviour of soft core sandwich beams subject to localized loads. At the material level, the soft core nonlinearity was investigated by many researchers. Zhu et al. (1997) and (1998) determined the effect of core material type and its density on the shape and nonlinearity of the stress-strain curve.

This paper presents an independent nonlinear strain compatibility model for the analysis of sandwich panels loaded in one-way bending, under concentrated or uniform loads. It accounts for geometric and material nonlinearities in the foam core and GFRP skins as well as excessive shear deformations. The model determines the load-deflection and load-strain responses of panels with composite skins and polyurethane cores of different densities as well as panels with ribs connecting the skins. The Winkler theory for beam on elastic foundation is incorporated in the model to capture the top skin behaviour under concentrated loads. The model is verified against experimental results and used in a comprehensive parametric study focussed on the effects of core density and skin thickness on the relative contributions of flexure and shear to deflections.

DESCRIPTION OF THE ANALYTICAL MODEL

A nonlinear analytical model is developed, accounting for material and geometric nonlinearities. The full stress-strain curves of the skins and foam core are considered. The total deflection is assumed to comprise three main components, one due to flexure, one due to shear deformation, and one due to the localized skin deflection under concentrated loads (Winkler effect). An incremental approach is used, where the concepts of force equilibrium and strain compatibility are satisfied in every loading step. The normal strain profile through the panel thickness is assumed to have a linear distribution (the effect of shear is accounted for separately). The numerical procedure is executed using FORTRAN90 code programming, and incorporated failure criteria that consider the following: *(a)* flexural tension or compression failure in the GFRP skins, *(b)* flexural tension or compression failure in the polyurethane core, *(c)* core shear (diagonal tension) failure, *(d)* GFRP ribs shear failure, or *(e)* skin wrinkling (local buckling). The model establishes the moment-curvature responses of cross-sections, which are terminated at a point governed by one of the five failure criteria discussed above (the one producing the lowest load capacity). The curvatures are integrated along the span to obtain the flexural deflection. The deflection due to shear deformation of the core and the localized top skin deflection are then added as will be discussed. The following sections provide a detailed description of different components of the model.

Strain Profile

The uncoupling of the flexural-induced and shear-induced deflections enables one to make the simplified assumption that the normal strain field varies linearly over the thickness. The two extreme fibre strains along with the zero strain point at neutral axis level are assumed to follow a straight line. Figure 1 shows the assumed linear strain profile through the sandwich panel thickness, which is expressed as follows:

$$\varepsilon_c = \varepsilon_t \left(\frac{H - y_{bar}}{y_{bar}} \right) \tag{1}$$

where ε_c and ε_t are the extreme fibre compressive and tensile strains, respectively. H is the overall cross-section height and y_{bar} is the neutral axis level measured from the extreme tension fibre.

Nonlinear Material Properties

Soft polyurethane foam cores are highly nonlinear materials, especially under compressive stresses, where the maximum compressive strain is almost 80%. Figure 2(a) shows the tensile and compressive normal stress-strain responses for a typical soft polyurethane foam as established by the first author, Sharaf (2010), through coupon tests. The shear behaviour of the polyurethane foam is characterized by very low shear rigidity as shown in Figure 2(b), also based on the coupon tests. The slight nonlinearity of [0/90] cross-ply GFRP is also taken into consideration for tension and compression (Figure 2(c)) along with the significant nonlinearity of the GFRP ribs in shear, arising from diagonal loading of the cross-ply rib (Figure 2(d)). In order to model the polyurethane foam and GFRP material constitutive relationships, a curve fitting technique is developed to track the average experimental stress-strain curve of a group of coupons for each case. The curve fitting technique is based on a cubic spline function concept developed by De Boor (2001). Details of the procedure can be found in the doctoral thesis of the first authors, Sharaf (2010).

Meshing

A layer-by-layer approach is adopted to integrate stresses over the cross-sectional areas of the GFRP skins and the polyurethane foam core. The cross-section is divided into three main parts, Part 1 to 3 (Figure 3). The model assumes a plain stress problem where a constant strain occurs across the width. Therefore, all layers extend the full width of the panel. The sandwich panel problem is very sensitive to shear and through-thickness compressibility of the soft core. Therefore, a sensitivity study is carried out and focussed on the through-thickness mesh refinement of the core. In the span direction, a large number of segments (160) was used and kept constant. Parts 1 and 3 are the GFRP skins and are represented by a single layer, each. In order to establish the appropriate number of layers for the core (Part 2) that leads to a converged solution, the convergence study was carried out using 2, 8, 12, 16, 20 and 24 layers within the depth of the core. The convergence study was carried out on the sandwich panels tested by Shawkat (2008), taking into account three different loading configurations: three-point bending (panel P1), four-point bending (panel P2) and a uniform loading configuration (panels P3 to P5). The converged solution was based on ultimate load, taking into consideration all the different failure criteria mentioned earlier for both the skins and core. Figure 4 shows the variation of the predicted failure load with number of layers, for different loadings (full details of analysis are given later). The figure shows that convergence depends slightly on the loading configuration. Panel P1 showed a minimal total variation in the predicted failure load of about 8% and the solution converged at 16 layers. Panel P2 showed a variation of 10% in the predicted failure load, and the solution converged also at 16 layers. Panels P3 to P5 required 20 layers to reach convergence and the predicted failure load variation was about 12%. As such, it was finally decided to use 20 layers within the core and two layers for the skins in the rest of the study. The 160 elements along the half span will be referred to as 'segments' while the 22 elements along the depth of the panel will be referred to as 'layers'.

Force Equilibrium and Moments

Figure 3 shows a cross-section of the sandwich panel under a given normal strain distribution at a given load. Only two independent parameters are needed to establish the complete strain profile, namely the strain at any level, say at the extreme bottom ε_t, and the neutral axis depth y_{bar}. The strain ε_i at any GFRP or polyurethane foam layer i, located at a distance y_i from the bottom extreme tension side, can then be determined from the linear strain distribution as follows:

$$\varepsilon_i = \varepsilon_t \left(\frac{y_{bar} - y_i}{y_{bar}} \right), \qquad \text{If } y_i \le y_{bar} \tag{2}$$

$$\varepsilon_i = \varepsilon_c \left(\frac{y_i - y_{bar}}{H - y_{bar}} \right), \qquad \text{If } y_i \ge y_{bar} \tag{3}$$

The normal stress in any element, either GFRP or polyurethane foam, σ_i is then calculated from the corresponding normal stress-strain curve, whether in tension or compression, using the cubic spline fitting curves. The total cross-section force at a given stage of loading (i.e. for a given ε_t and ε_c) can be obtained by numerical integration of stresses over the cross-section, for both GFRP and polyurethane, which must equal to zero in flexure to satisfy equilibrium, as follows:

$$\sum_{GFRP,i=1}^{n} (\sigma_{Si}\ A_{Si}) + \sum_{PolyurethanFoam,i=1}^{n} (\sigma_{Ci}\ A_{Ci}) = 0 \quad (4)$$

The corresponding moment M is calculated as follows:

$$M = \sum_{GFRP,i=1}^{n} (\sigma_{Si}\ A_{Si}\ y_i) + \sum_{PolyurethanFoam,i=1}^{n} (\sigma_{Ci}\ A_{Ci}\ y_i) \quad (5)$$

where σ_{Si} and σ_{Ci} are the stresses in skins or core at layer i, respectively, n is the total number of layers. A_{Si} and A_{Ci} are the cross-sectional areas of the GFRP or polyurethane layer i, respectively, and y_i is the distance between the centroid of layer i and the bottom extreme fibre.

The presence of longitudinal and transverse ribs is accounted for in the internal forces. At each cross section, the specific width and thickness of the longitudinal or transverse rib was considered. Also, the contribution of the web of the rib in each layer i is considered.

Moment-Curvature Response

The aforementioned concepts and geometric relationships have been used to establish the moment-curvature response of a given cross-section in the panel. A computer code was written in FORTRAN90. The program can deal with any material stress-strain curve of any shape. A simplified flowchart illustrating the procedure is provided in Figure 5. The moment-curvature algorithm can be summarized as follows:

1. Input panel dimensions, overall thickness, skin thickness, loading span, and loading pattern.
2. Divide the core into n numbers of layers (in this study it was shown that $n = 20$ for the core is sufficient). Each skin counts as one layer.
3. Define the stress-strain relationships for both GFRP and polyurethane foam materials in tension, compression and shear.
4. Assume a strain value at the top surface of the sandwich panel, ε_c, (Figure 3) less than the ultimate strain of GFRP in compression, ε_{cu}.

5. Assume a neutral axis depth from bottom surface, y_{bar} (Figure 3).
6. Calculate the corresponding tensile strain ε_t at the bottom skin (Eq. 1). Check that this strain does not exceed GFRP ultimate tensile strain GFRP, ε_{tu}, otherwise tension failure has occurred.
7. Construct the linear strain profile by calculating ε_i from Eqs. 2 and 3 at each layer *i* (Figure 3). It is worth noting that the ultimate tensile strain of the foam core, in tension or compression, are significantly higher than those of GFRP skin (Figure 2). As such, it is not possible for the extreme layers of foam core to fail in the longitudinal direction before GFRP skins.
8. Calculate the corresponding stresses, σ_{Si} and σ_{Ci}, in the GFRP skins and foam core, respectively (Figure 1), using material stress-strain relationship through the cubic spline functions.
9. For each layer *i* in the cross-section, calculate its cross-sectional area, A_i, weather it is A_{Si} (for the GFRP skins) or A_{Ci} (for the polyurethane foam core).
10. Calculate the tensile and compressive forces induced in each layer, $(\sigma_{Si} A_{Si})$ or $(\sigma_{Ci} A_{Ci})$.
11. Check equilibrium by summing the tension and compression forces (Eq. 4). If the total force sum is not equal to zero, return to Step 5 and assume a new neutral axis depth. Continue the process and repeat until equilibrium is satisfied.
12. Determine the moments of the forces in all layers about neutral axis. The summation of all moments is the total moment M (Eq. 5) for the strain ε_c applied in Step 4.
13. Compute the curvature as $\psi = \varepsilon_t / y_{bar}$.
14. Return to Step 4 and assume a new strain. Repeat this process until the ultimate strain of GFRP skins is reached in tension or compression and the complete M-ψ response is developed.

Generation of Full Load-Deflection Response

The load-deflection response consists of three components, namely a flexural component, a shear component, and a local skin Winkler effect component. In typical structural materials such as steel and concrete beams, deflections are dominated by the flexural contribution only. However, in sandwich panels with soft cores, the shear contribution is quite significant. In addition, Winkler effect under concentrated loads must be considered. Figure 6 shows a flow chart for the procedure of obtaining the complete load-deflection response. Details are explained as follows:

Flexural effect: Once the M-ψ response of the cross-section is obtained, the load-deflection response can be estimated for a given loading scheme. The mid-span deflection of the panel (δ_m) under symmetric loading is calculated by integrating the curvatures (ψ) along the span using the moment-area method (Ghali and Neville, 1989), as given by the following equations:

$$\delta_m = \iint \psi(x)dxdx \tag{6}$$

To start the process, an initial load is assumed and one half of the span is divided into several segments (160 in this study), each segment l has a length dx. The average bending moment experienced within each of the segments (M_i) is calculated for the applied load. The previously established moment-curvature response is then used to determine the average curvature corresponding to M_i within each segment (ψ_i). The product ($\psi_i\, dx$) gives the change in slope ($\Delta\theta_i$) of the deformed segment. For symmetric geometry and loading, the slope of the deformed member at mid-span is zero, and the slope at midpoint of each segment (θ_i) is equal to the summation of $\Delta\theta_i$ for all segments between mid-span and the point of interest. The product ($\theta_i\ dx$) gives the change in deflection (Δy_i) of the segment. The summation of Δy_i values for all segments between mid-span and the support gives the total mid-span deflection of the panel (δ_m). This entire process is repeated at various load levels in order to establish the first component of load-deflection curve, which is due to flexure only.

Shear effect: The deflection of any segment l along the span, and at a layer i along the depth, due to shear stress, $\delta_{v,l,i}$, is equal to:

$$\delta_{v,l,i} = \gamma_{l,i}\ dx \tag{7}$$

where the shear strain $\gamma_{l,i}$ can be calculated from the shear stress $\tau_{l,i}$ at a specific layer i and a given segment l under a specific loading conditions, as shown in Figure 7. Segment l varies from 1 to 160 and i varies from 1 to 22. The shear stress $\tau_{l,i}$ can be calculated as follows:

$$\tau_{l,i} = \frac{V_l \, Q_{t,l,i}}{I_{t,l} \, b_{t,l,i}} \tag{8}$$

where V_l is the shear force at segment l and $Q_{t,l,i}$ is the first moment of area for the transformed cross-section about neutral axis, at specific layer i. $I_{t,l}$ is the moment of inertia for the transformed cross-section and $b_{t,l,i}$ is the width of the transformed cross-section at layer i. The transformed section is established by transforming the width $b_{l,i}$ of each skin or core layer i at any segment l to a unified core material based on the modulus of the foam in compression, as follows:

$$b_{t,l,i} = b_{l,i} \frac{E_{l,i}}{E_{fc}} \tag{9}$$

where $b_{l,i}$ is the original width at segment l for layer i and $b_{t,l,i}$ is the transformed width. $E_{l,i}$ is the secant modulus of elasticity of the normal stress-strain curve of the polyurethane or GFRP, in tension or compression (depending on the location of layer i relative to neutral axis), at segment l. $E_{l,i}$ is established from the material curve at the specific normal strain $\varepsilon_{l,i}$ of layer i at segment l at this particular loading. E_{fc} is the reference modulus which is the initial modulus of the polyurethane foam in compression. Figure 8 shows the original and the transformed cross-sections, respectively.

After calculating shear stress, the corresponding shear strain $\gamma_{l,i}$ can be calculated using the core material shear stress-strain curve and is used to compute the shear deflection of layer i. To calculate the total shear deflection of layer i at mid-span of the panel, the shear deflection for each segment ($l = 1 \text{ to } 160$) should be summed in the longitudinal direction of the panel.

$$\delta_{v,i} = \sum_{l=1}^{m=160} \gamma_{l,i} \, dx = \sum_{l=1}^{m=160} \delta_{v,l,i} \tag{10}$$

where $\delta_{v,i}$ is the total shear deflection of layer i specifically at mid-span, and m is the total number of segments along the half span (160). As such, at every layer i, the shear deflection values will be different from one layer to the other, which is obviously impossible because each layer is joined to the adjacent layers and the whole cross-section must be continuous, without any gaps or overlaps (Shanley, 1957). As a result, each layer will rotate clockwise (or counter-clockwise) to adjust the cross-section continuity at this segment (Figure 7). This rotation causes the cross-section to warp, which means the cross-section will not remain plane. On the other hand, the calculated bending deflections were based on the beam theory, assuming plane sections remain plane after deformation. However, it has been found that the assumption that plane sections remain plane after deformation can be used with negligible errors in most cases (Shanley, 1957).

The top skin deflection due to shear forces at any segment, $\delta_{v,l,top}$ can be assumed as the average deflection of all layers above the neutral axis, while the bottom skin deflection at the same segment, $\delta_{v,l,bot}$, is the average deflection of all layers below the neutral axis, as follows:

$$\delta_{v,l,top} = \sum_{i=1}^{n_{top}} \delta_{v,l,i} \Big/ n_{top} \qquad \delta_{v,l,bot} = \sum_{i=1}^{n_{bot}} \delta_{v,l,i} \Big/ n_{bot} \tag{11}$$

where n_{top} is the number of layers above the neutral axis and n_{bot} is the number of layers below the neutral axis. The total shear deflections at the panel mid-span, for both skins, are:

$$\delta_{v,top} = \sum_{l=1}^{m=160} \delta_{v,l,top} \qquad \delta_{v,bot} = \sum_{l=1}^{m=160} \delta_{v,l,bot} \tag{12}$$

where $\delta_{v,top}$ and $\delta_{v,bot}$ are the total top and bottom skin deflections due to shear, at the panel mid-span, respectively. The two skins will not deflect equally because of the soft core and the difference represents a change in thickness of the panel at this loading step, which is discussed in detail later. In panels with GFRP ribs, the effects of longitudinal and transverse ribs on the transformed section analysis are considered at each cross section. This is considered in calculating $b_{t,l,i}$ in Eq. 9, in calculating $I_{t,l}$ used in Eq. 8 and in calculating $Q_{t,l,i}$, also used in Eq. 8.

Winkler effect: Because of the soft core, loads applied to the top skin will cause local bending and deflection. To capture this effect, the concept of beam on elastic foundation is employed. It is based on the assumption by Winkler that the reaction forces at every point are proportional to the deflection of the beam (skin) at that point (Hetenyi, 1946). In sandwich panels, the top skin can be considered as a beam resting on elastic foundation based on the compressibility of the foam core (Figure 9). Note that in in panels with GFRP ribs, the ribs were considered rigid enough to prevent the localized effect caused by the softness of the core. The general differential equation for the deflection curve of a beam on elastic foundation is:

$$EI\frac{d^4w}{dx^4}+kw=0 \tag{13}$$

where w is the vertical deflection and EI is the flexural rigidity of the top skin. k represents the elasticity "modulus" of the polyurethane foam core. The general solution of this equation is:

$$w=e^{\beta x}\left(C_1\cos\beta x \quad + \quad C_2\sin\beta x\right) \quad + \quad e^{-\beta x}\left(C_3\cos\beta x \quad + \quad C_4\sin\beta x\right) \tag{14}$$

where:

$$\beta=\sqrt[4]{\frac{k}{4EI}} \tag{15}$$

and C_1 to C_4 are the integration constants and can be calculated by the applied boundary conditions. Because of the fact that the skin does not have an infinite length but limited to the panel span, the superposition method developed by Hetenyi (1946) is used. The superposition method is based on determining the skin end forces (bending moments and shear forces) which will transform the infinite length beam to a finite length beam with a specific span. The solution of both concentrated and uniform load cases with finite length has been presented in Sharaf (2010).

Superposition: The addition of the compressive stresses resulting from the Winkler's local bending in the top skin, to the original flexural compressive stresses, was considered to get the total skin stress. Also, the final top skin deflection is the sum of all three deflections as follows:

$$\delta_{tot,l} = \delta_{m,l} + \delta_{v,l,top} + \delta_{w,l} \tag{16}$$

where $\delta_{m,l}$, $\delta_{v,l}$ and $\delta_{w,l}$ are deflections at segment l due to flexure, shear and elastic foundation, respectively. The Winkler effect is neglected in the bottom skin at the support regions.

Nonlinear Geometric Effects

As indicated earlier, the shear stress variation across the sandwich panel thickness results in the shear deflection also being variable through the thickness. As such, each layer will deform (skew) in a value different from the adjacent layers. Also, because of the different polyurethane core behaviour in tension and compression and material nonlinearity, the layers below neutral axis will have different transformed widths from the layers above. Furthermore, Winkler effect will compress the core and reduce the total thickness of the panel. All this will result in different values of deflection for the top and bottom layers (Eq. 12). This difference will cause the cross-section to be "squeezed" at the end of the loading step and a smaller thickness is used under the next load increment (Figure 7). In order to account for this geometric nonlinearity, the neutral axis location of the new transformed section has to be re-established in each load step, for each segment along the span. After applying the first load increment, the resulting deflection is calculated for both flexure and shear at each segment. Then, the new section thickness $H_{new,l}$ is calculated using Eq. 17, at each segment. A new location of neutral axis is then recalculated at each segment.

$$H_{new,l} = H_{old,l} - \left|\delta_{v,top,l} - \delta_{v,bot,l}\right| - \delta_{w,l} \tag{17}$$

where $H_{old,l}$ is the cross-section thickness at the previous load increment. A new moment-curvature relationship at every segment is established for the section with the new thickness, as explained earlier, using the developed cubic spline material curves. Then, under any moment value at each segment along the span, the corresponding curvature is calculated. As the curvature values for every segment at certain load increment is known, the deflection due to moment can be calculated at this load increment. Also, the moment-strain (tensile or compressive) relationships at any segment, at a certain load increment, can be found.

Failure Criteria

Seven main failure criteria were considered, namely *(1)* a flexural tension failure of GFRP skin, *(2)* a compression failure of GFRP skin by crushing, *(3)* a shear failure of the foam core, *(4)* a shear failure of the GFRP rib, *(5)* a tension failure of the foam core, *(6)* a compression failure of the foam core by excessive deformation, and *(7)* a wrinkling failure (local buckling) of the GFRP compressive skin. The tension failure of the GFRP skin is highly unlikely as the compression skin or core shear failure usually governs. Six of the failure criteria are material failures and are governed by the stress-strain curves established earlier. The seventh failure criterion, namely the compression skin wrinkling under flexural stresses is based on the model by Allen (1969), Eq. 18:

$$\sigma_{cr} = B_1\, E_S^{\frac{1}{3}}\, E_C^{\frac{2}{3}} \quad \text{and} \quad B_1 = 3\left[12\left(3-\nu_c\right)^2\left(1+\nu_c\right)^2\right]^{-\frac{1}{3}} \tag{18}$$

where σ_{cr} is the minimum critical wrinkling stress of skin, E_S is the skin longitudinal compressive modulus, E_C is the core compressive modulus and ν_c in the core Poisson's ratio. Throughout the formulation of the moment-curvature response, the maximum values of compressive and tensile strains in the skins are continuously monitored, to detect any flexural or wrinkling failures. Also, shear failure is defined when the shear stresses in the shear analysis algorithm exceed the failure values of the polyurethane foam core or the GFRP ribs.

Illustration of Key Features of the Model

The model developed has several significant features, namely, accounting for the geometric non-linearity, which is the change in thickness due to core compressibility, significant material non-linearity of polyurethane foam core, and a number of possible failure criteria of GFRP and polyurethane. Also, the model is capable of displaying individually the different components of deflection produced by flexure, shear, and localized loading of the skin according to beam on elastic foundation principles. In order to illustrate the significance of these features, the load-deflection responses of the test specimens (Shawkat, 2008) with two different core densities are predicted under five different conditions: In case (1), the model neglects material nonlinearity of foam and GFRP, geometric nonlinearity and beam on elastic foundation. In this case, the stiffness based on the initial linear parts of the stress-strain curves were used as constants throughout the analysis. In case (2), only the material nonlinearity is considered for both GFRP and Polyurethane foam, in tension, compression, and shear. In case (3), in addition to material nonlinearity, geometric nonlinearity is also considered. In case (4), in addition to material and geometric nonlinearities, core compressibility under the loads is considered through Winkler effect. Case (5) is essentially case (4) but with applying the failure criteria.

Figures 10(a) and (b) show the experimental and the analytical responses for the five cases for specimens P3 to P5 with soft cores of 32 kg/m^3 density, and specimens P7 to P9 with denser cores of 64 kg/m^3, respectively. The figures clearly show that ignoring material nonlinearity, case (1), grossly underestimate deflection, especially at higher loads. Considering material nonlinearity but ignoring geometric nonlinearity, case (2), provides significant improvement of prediction throughout the loading history but still underestimates deflection at higher loads for the softer core specimens (Fig. 10(a)). Accounting for geometric nonlinearities, case (3), and considering the Winkler effects, case (4), slightly improves prediction, especially for softer core specimens. Case (5), which enables failure criteria, leads to the final prediction with the full capabilities of the model and shows reasonable agreement with the experimental responses. Clearly, the most important effect is the material nonlinearity (i.e. case (1) versus case (2)). An illustration of the individual contributions of flexure, shear and Winkler effect to deflections is presented next.

Model Validation

The analytical model is validated using the load-deflection and load-longitudinal strain responses of ten sandwich panels tested by Shawkat (2008), including low density core (32 kg/m^3) panels (Fig. 11) and high density core (64 kg/m^3) panels (Fig. 12). Figure 11(a) shows the responses of panel P1 tested in three-point bending. The figure shows good agreement between measured and predicted load-deflection responses, except for deflection at ultimate, which was slightly overestimated. It is clear from the figure that shear deflection is significantly higher than the flexural deflection. For the load-strain responses, although the model accounts for the Winkler effect in terms of deflection and localized bending stresses of the skin, it could not fully capture the excessive compressive strain of the loaded skin at the wrinkle location. The reason is that the strain at the point of maximum inward wrinkling was beyond the ultimate compressive strain obtained from the GFRP compression coupons tests. The model predicts the correct failure mode at ultimate, which is the compression failure of the foam core under the load. This is detected by approaching the flat plateau of stress-strain curve of the foam under the load. This in turn leads to excessive thickness reduction of cross-section in the vicinity of load, which triggered a shear failure adjacent to the load. Although failure appears similar to a local buckling, it is actually excessive deformation of the core, as the critical skin stress σ_{cr} (Eq. 18) was not reached.

Figure 11(b) shows the responses of panel P2 tested in four-point bending, which showed reasonable agreement. It is to be noted that the deformed shape of panel P2 during testing was not symmetric as deflection under one load was slightly higher than the other, and indeed triggered failure to occur at that loading point. The model predicted correctly the failure mode, which was compression failure of the foam core under the loading point by excessive deformation, leading to shear failure as indicated for panel P1. Unlike P1, the deflection at mid-span due to the Winkler effect is zero because the loads are relatively far from mid-span.

Figure 11(c) shows the responses of identical low-density core panels P3 to P5 tested under uniformly distributed load (8 point loads), while Fig. 12 shows the responses of identical high-density core panels P7 to P9, also tested under 8 point loads. Very good agreement is observed. The model also predicted the correct failure modes in both cases, namely shear failure of the core. Figure 11(c) shows that the shear deflection is significantly larger than the flexural deflection, because of the low-density core, whereas Figure 12 shows that both flexural and shear deflections are somewhat similar in high-density core. At a given load level, the shear deflection is significantly lower for high-density core than for low-density core.

PARAMETRIC STUDY

In this section, a parametric study is conducted to study the two most influencing parameters affecting sandwich panel behavior, namely skin thickness and polyurethane core density. The core densities are varied from M1=32 kg/m^3 to M6=192 kg/m^3 at 32 kg/m^3 intervals. The top and bottom skin thicknesses studied are t1=1.6 mm, t2=3.2 mm, and t3=4.8 mm. The dimensions of the sandwich panel used in the parametric study are 1500x300x78 mm, and the panel is assumed to be loaded with a uniform pressure over a span of 1400 mm. The overall panel thickness is kept constant at 78 mm. Figure 13 shows the stress-strain curves of the polyurethane of different densities in compression, tension and shear. The curves were developed analytically by the first author (Sharaf, 2010) using the technique suggested by Gibson and Ashby (1988).

Table 1 summarizes the parametric study and results, including failure modes. For each of the six core densities, the three skin thicknesses are used, giving a total of 18 cases. Each case is given a specific ID. Figures 14(a) to (f) show the load-deflection responses of six out of the 18 panels, namely, the ones with the lowest (M1) and highest (M6) core densities. The figures also show the individual contributions of flexure, shear and Winkler effect to total deflection. It can be immediately seen from the figures that the shear deflection reduces significantly as core density increases, while the flexural deflection contribution increases. The Winkler effect is very small for all densities because the load is uniformly distributed, unlike the case of concentrated load (Figure 11(a)), where it was quite pronounced.

Effect of Skin Thickness

Figures 15(a) to (c) show the effect of skin thickness on ultimate load, stiffness, and percentage of flexural contribution to total deflection. It can be seen from Figure 15(a) that increasing the skin thickness does not always lead to a significant increase in ultimate load. For example increasing the skin thickness from 1.6 mm to 3.2 mm enhanced the ultimate strength for all core densities, at various degrees, except for M1, which was not affected. On the other hand increasing the thickness from 3.2 mm to 4.8 mm enhanced the strength significantly for the M3 and M4 densities only. The reason is that for those two foam densities the failure mode was skin compression not a core shear failure. Figure 15(b) shows that the stiffness generally increases as the skin thickness increases, except for the very low density core M1 which was not affected. Figure 15(c) shows that the contribution of flexural deflection to the total deflection consistently reduces as the skin thickness increases. In general, one can conclude that increasing skin thickness becomes more effective, particularly for strength, as core density increases up to a certain level, the M4 density in this case.

Effect of Core Density

Figures 16(a) to (c) show the effect of core density on ultimate load, stiffness, and percentage of flexural contribution to total deflection, respectively. Increasing the density enhances flexural strength up to a certain level, namely the M4 density. Beyond this, the strength may reduce again or stabilizes. This behaviour is a result of changing failure mode from core shear failure to skin compression failure and then core shear failure again. Also, increasing the density generally enhances stiffness, but at a lower rate beyond a certain density (M3). The contribution of flexural deflection certainly increases considerably as density increases but at a smaller rate beyond density M3. It appears from this study that perhaps the optimal core density for strength is the (M3-M4) range of 96 to 128 kg/m^3. This range represents the lowest density necessary to achieve the highest ultimate strength and stiffness. Furthermore, this range of density combined with the largest skin thickness used, 4.8 mm, resulted in the highest level of strength (i.e. cases M3t3 and M4t3).

CONCLUSIONS

In this study, a nonlinear analytical model was developed to study the flexural behaviour of sandwich panels composed of a polyurethane foam core and GFRP skins. The FORTRAN-coded analytical model accounted for both material and geometric nonlinearities. The model was based on equilibrium and strain compatibility, accounting for excessive shear deformations and thickness reduction due to soft core. The model captured the localized deformations of the loaded skin using beam-on-elastic foundation principles. The model is also able to isolate, and present separately, the individual contributions of flexure, shear, and localized skin deformations, to the overall deflection of the panel. The model was successfully validated using experimental results.

A sensitivity study using the model showed that the most important features in the model are accounting for material non-linearity of the core and enforcing the proper failure criteria. A parametric study was also performed to examine the effects of core density and skin thickness and concluded the following:

1. As the core density increased from 32 to 192 kg/m^3 the contribution of shear to the overall deflection reduced from about 90 to 10%.
2. For a very low density core (32 kg/m^3), increasing the skin thickness has an insignificant effect on flexural strength and stiffness, as failure is consistently governed by core shear failure.
3. As the core density increases, failure mode changes from core shear to compressive skin failure associated with an increase in strength and stiffness. At large skin thicknesses, this trend could revert to core shear failure and is then associated with reduction in strength.
4. As the core density increases, increasing the skin thickness becomes more effective, leading to enhancement in strength and stiffness, but only up to a certain core density.
5. It appears that the optimal core density of the sandwich panels is within the 96 to 128 kg/m^3 range. This represents the lowest density necessary to achieve the highest strength and stiffness.

REFERENCES

Allen, H. G. (1969). Analysis and design of structural sandwich panels. Pergamon Press, Oxford, London, England.

Chandrashekhara, K., and Krishnamurthy (1990), “Free vibration of composite beams including rotary inertia and shear deformation." Composite Structures, 14, 269-279.

De Boor, Carl (2001). “A Practical Guide to Splines.” Springer-Verlag, New York.

Frostig, Y., and Baruch, M. (1990). “Bending of sandwich beams with transversely flexible core.” AIAA Journal, 28(3), 523-531.

Frostig, Y., Baruch, M., Vilnay, O., and Sheinman, I. (1992). “High-order theory for sandwich-beam behavior with transversely flexible core.” Journal of Engineering Mechanics, 118(5), 1026-1043.

Frostig, Y. (1993). “On stress concentration in the bending of sandwich beams with a transversely flexible core.” Composite Structures, 24(2), 161-169.

Frostig, Y., Thomsen, O. T., and Sheinman, I. (2005). “On the non-linear high-order theory of unidirectional sandwich panels with a transversely flexible core.” International journal of solids and structures, 42(5), 1443-1463.

Ghali, A. and Neville, A. M. (1989). Structural analysis: A unified classical and matrix approach, 3rd Ed., Chapman and Hall, London and New York.

Gibson L.J. and Ashby M.F. (1988). Cellular solids: structure and properties. Oxford: Pergamon Press.

Hetenyi, M. (1946). “Beams on Elastic Foundation, Theory with Applications.” Ann Arbor: The University of Michigan press.

Holt, P. J., and Webber, J. P. H. (1982). “Exact solutions to some honeycomb sandwich beam, plate, and shell problems.” The Journal of Strain Analysis for Engineering Design, 17(1), 1-8.

Kant, T., and Patil, H. S. (1991). “Buckling load of sandwich columns with a higher order theory.” J. Reinforced Plastics and Composites, 10(1), 102-109.

Kant, T., and Mallikarjuna. (1989). “A high-order theory for free vibration of unsymmetrically laminated composite and sandwich plates-finite element evaluation.” Computers and Structures, 32(5), 1125-1132.

Ogorkiewicz, R. M., and Sayigh, A. A. M. (1973). “Deflection of carbon fibre/acrylic foam sandwich beams.” Composites, 4(6), 254-257.

Pearce, T. R. A. (1973). “The stability of simply-supported panels with fibre reinforced face plates.” Ph.D. Thesis presented to the University of Bristol, at Bristol, UK.

Senthilnathan, N. R., Lim, S. P., Lee, K. H., and Chow, S. T. (1988). “Vibration of laminated orthotropic plates using a simplified higher order deformation theory.” Composite Structures, 10, 211-229.

Sharaf, T. (2010). “Flexural behaviour of sandwich panels Composed of polyurethane core and GFRP skins and ribs.” Ph.D. Thesis, Queen’s University, Canada.

Shawkat, W. (2008). “Hybrid Members Employing FRP Skins Reinforcement for Beams and Cladding Wall Applications” A Master Thesis, Queen’s University, Canada.

Shanley, F.R. (1957). “Strength of Materials.” McGraw-Hill book company, Inc.

Shen, H., Sokolinsky, V. S., and Nutt, S. R. (2004). “Accurate predictions of bending deflections for soft-core sandwich beams subject to concentrated loads.” Composite Structures, 64(1), 115-122.

Zhu, H. X., Mills, N. J., and Knott, J. F. (1997). “Analysis of the high strain compression of open-cell foams.” Journal of the Mechanics and Physics of Solids, 45(11), 1875-1904.

Zhu, H., and Mills, N. J. (2000). “The in-plane non-linear compression of regular honeycombs. International Journal of Solids and Structures.” 37(13), 1931-1949.

Table 1. Summary of the parametric study and results

Core density	Skin Thickness (mm)	ID	P_u (kN)	%age Gain	k (kN/mm)	%age Gain	δ (mm)	%age Reduced	Failure mode
M1 (32 kg/m³)	1.6	M1t1	8.0	------	0.263	------	53.27	------	S
	3.2	M1t2	7.8	-2.5	0.293	11.85	47.25	11.30	S
	4.8	M1t3	7.6	-5.0	0.302	15.22	41.86	21.42	S
M2 (64 kg/m³)	1.6	M2t1	20.0	150	0.492	87.69	51.55	3.23	S
	3.2	M2t2	26.4	230	0.806	207.23	62.61	-17.53	S
	4.8	M2t3	25.6	220	0.907	245.87	46.51	12.69	S
M3 (96 kg/m³)	1.6	M3t1	21.6	170	0.916	249.24	27.82	47.78	C
	3.2	M3t2	38.4	380	1.534	484.93	35.39	33.56	C
	4.8	M3t3	56	600	1.975	653.09	42.28	20.63	C
M4 (128 kg/m³)	1.6	M4t1	21.6	170	0.998	280.30	25.23	52.64	C
	3.2	M4t2	40.8	410	1.744	564.98	28.89	45.77	C
	4.8	M4t3	57.6	620	2.308	779.80	34.17	35.86	C
M5 (160 kg/m³)	1.6	M5t1	22.4	180	0.998	280.46	25.1	52.88	C
	3.2	M5t2	42.0	425	1.647	528.09	28.9	45.75	C
	4.8	M5t3	44.4	455	2.368	802.96	21.81	59.06	S
M6 (192 kg/m³)	1.6	M6t1	22.4	180	1.034	294.14	24.67	53.69	C
	3.2	M6t2	34.8	335	1.908	627.34	20.85	60.86	S
	4.8	M6t3	33.6	320	2.618	898.18	13.91	73.89	S

P_u = Ultimate load
K = Stiffness
δ = Deflection at ultimate
CS = Polyurethane foam core shear failure
SC = GFRP top skin crushing failure

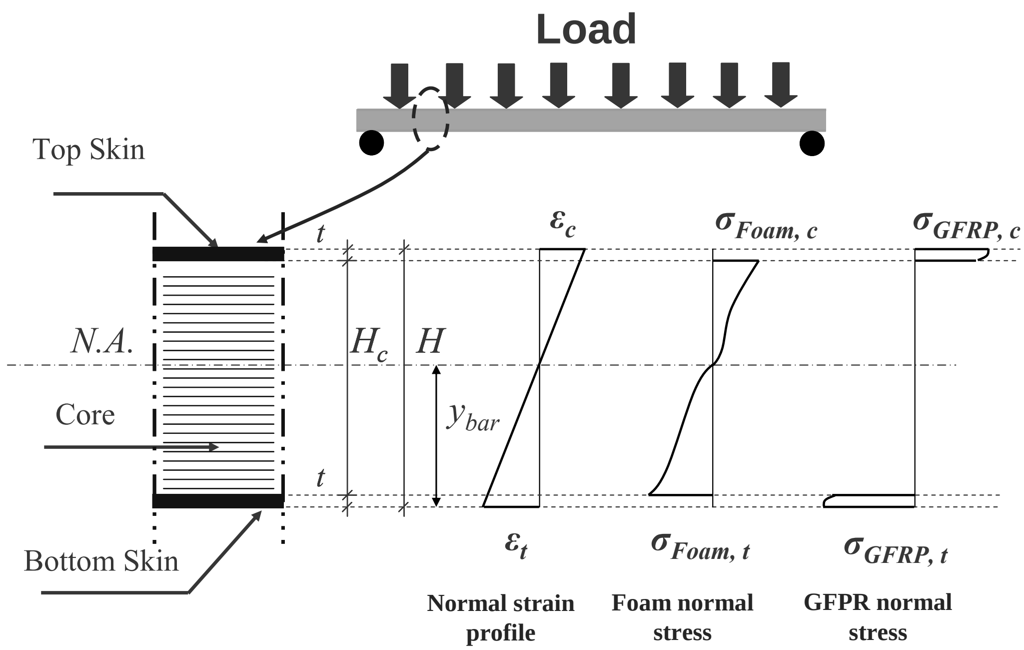

Figure 1. Normal stress and strain distributions

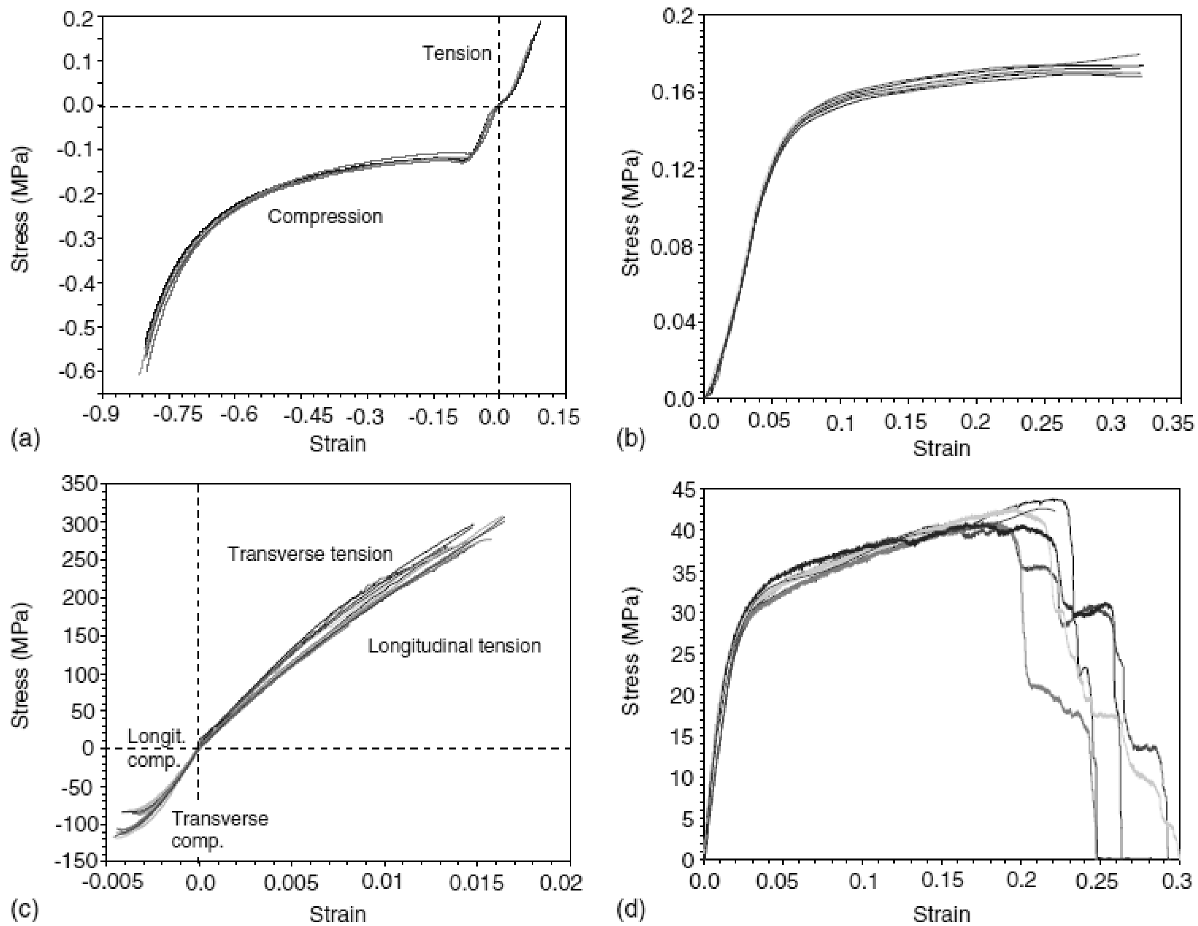

Figure 2. Stress-strain curves of sandwich panel materials tested by Sharaf (2010): (a) polyurethane core in tension and compression; (b) polyurethane core in shear; (c) GFRP in tension and compression; and (d) GFRP in shear.

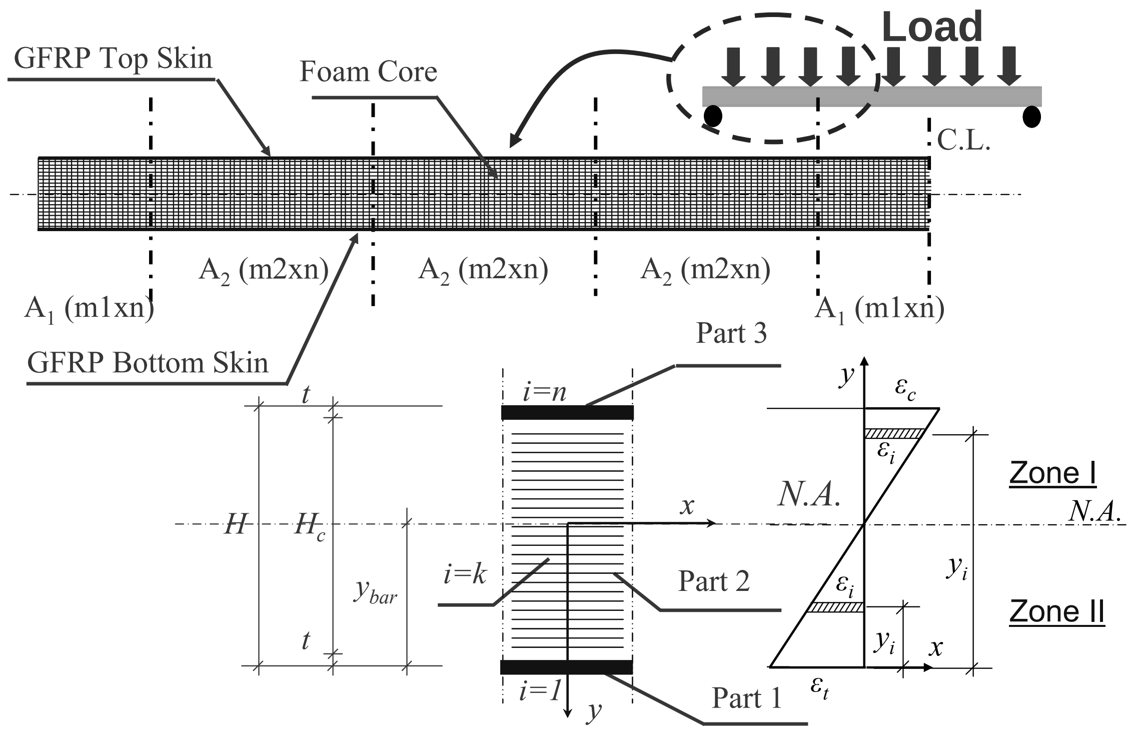

Figure 3. Meshing configuration of sandwich panels

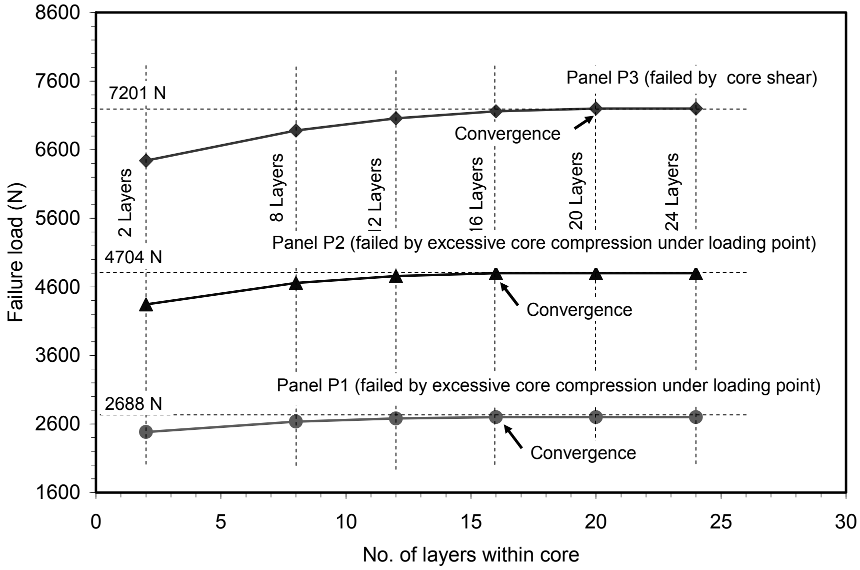

Figure 4. Variation of failure load with number of cross-section layers within core for the convergence study on specimen tested by Shawkat (2008)

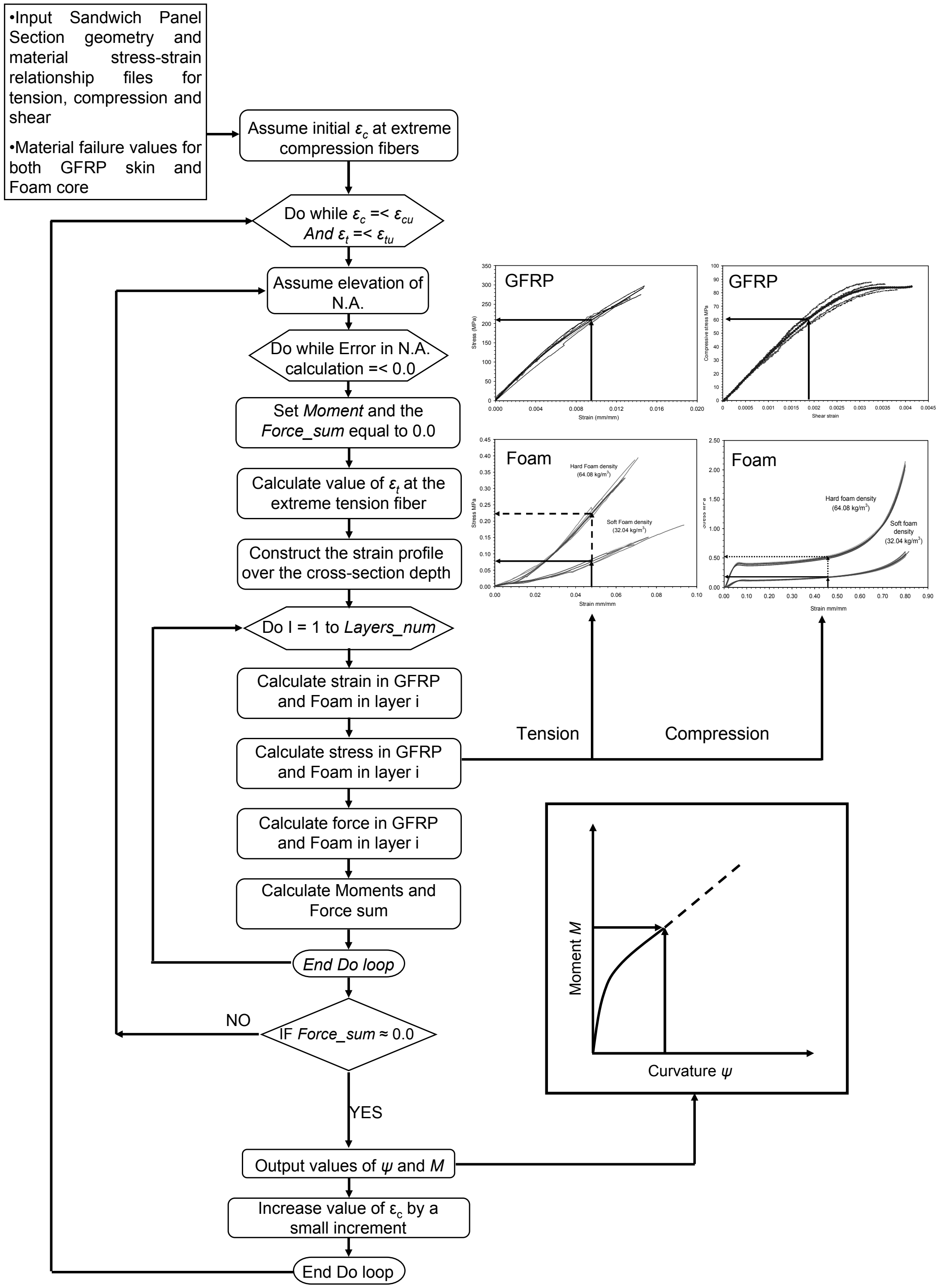

Figure 5. Flow chart of the procedure to obtain the moment-curvature response of a cross-section

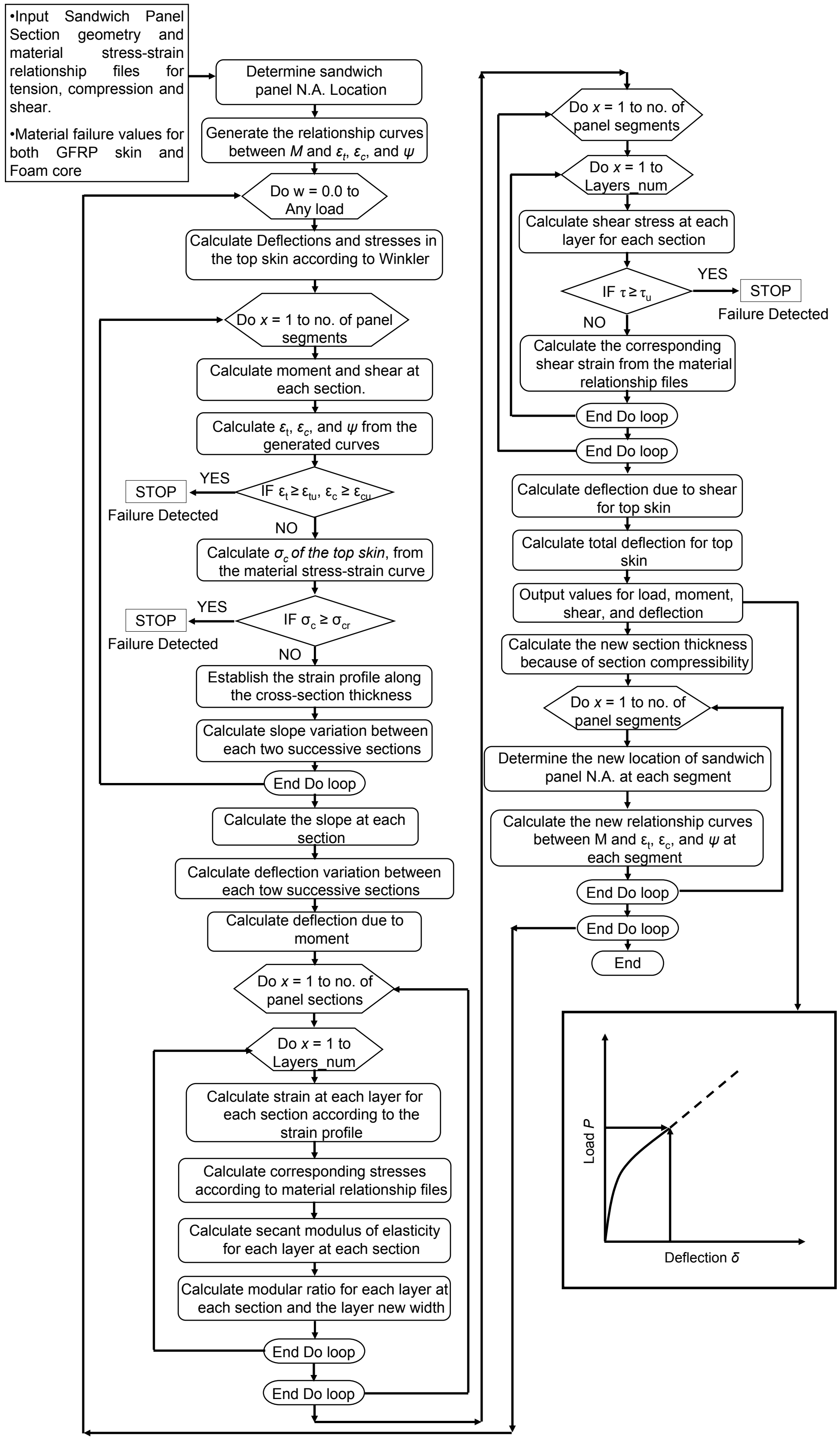

Figure 6. Flow chart of procedure used to obtain the load-deflection response

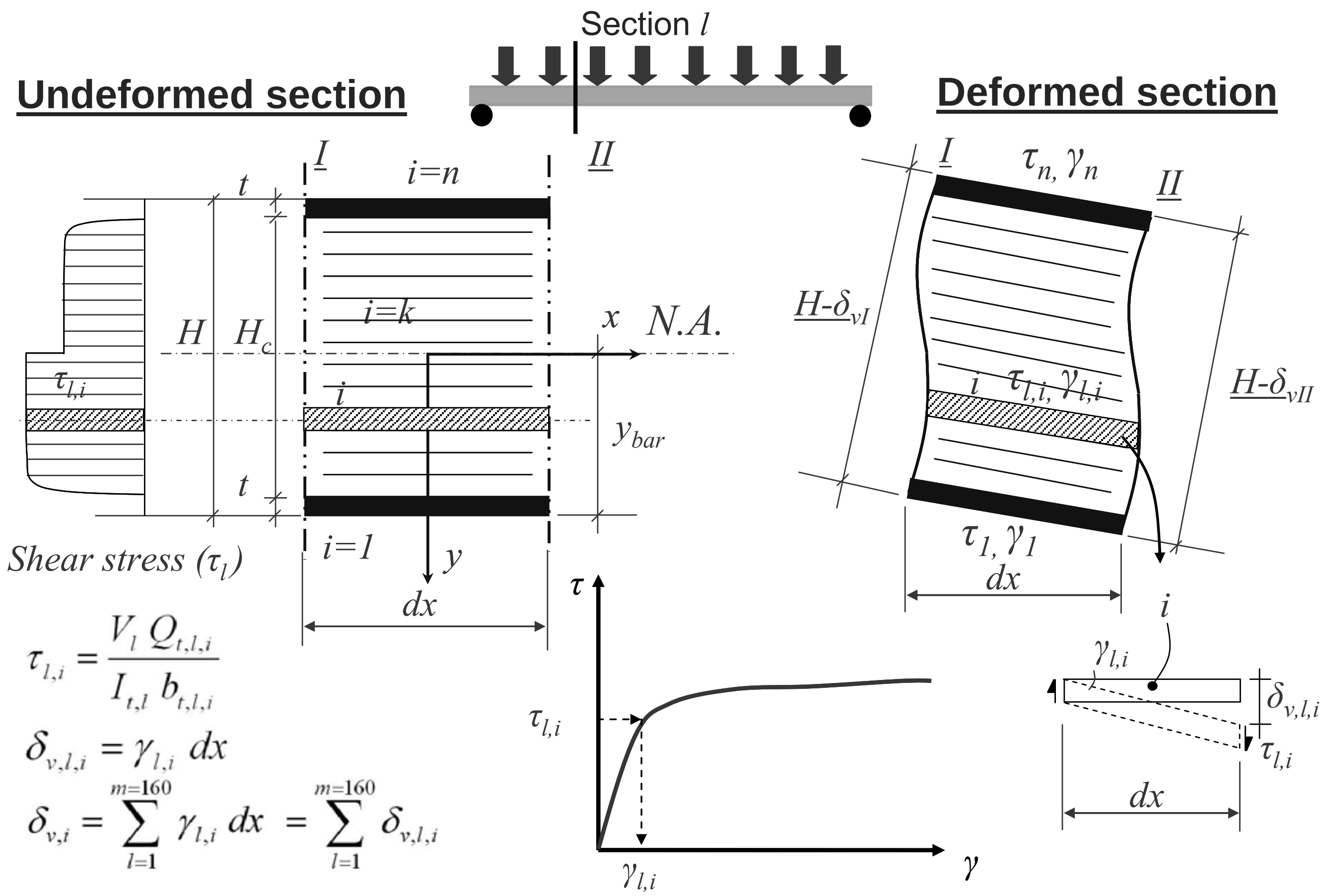

Figure 7. Shear deflections in sandwich panel

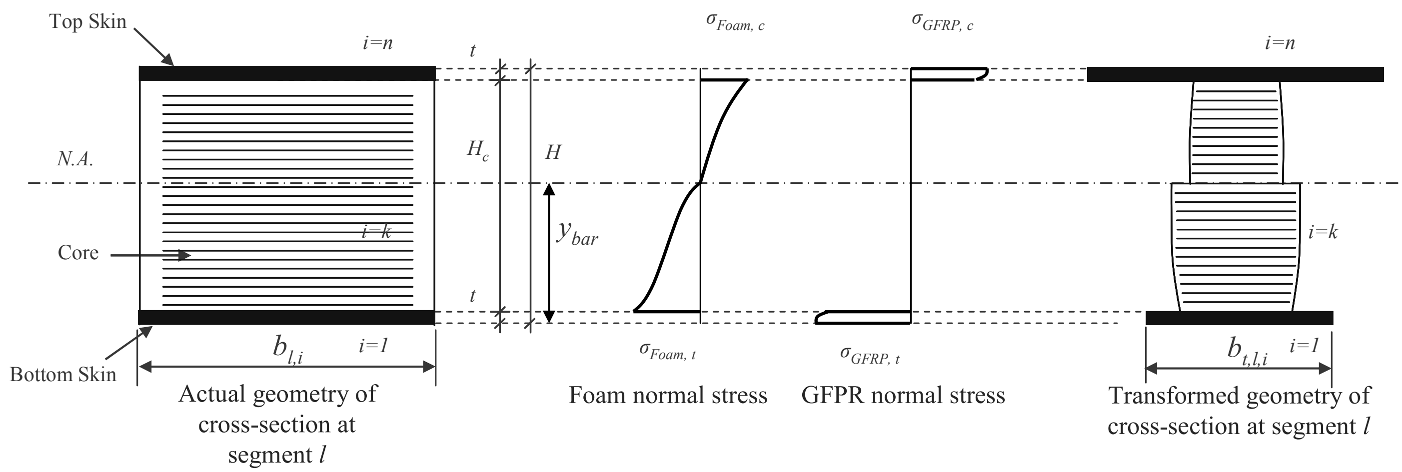

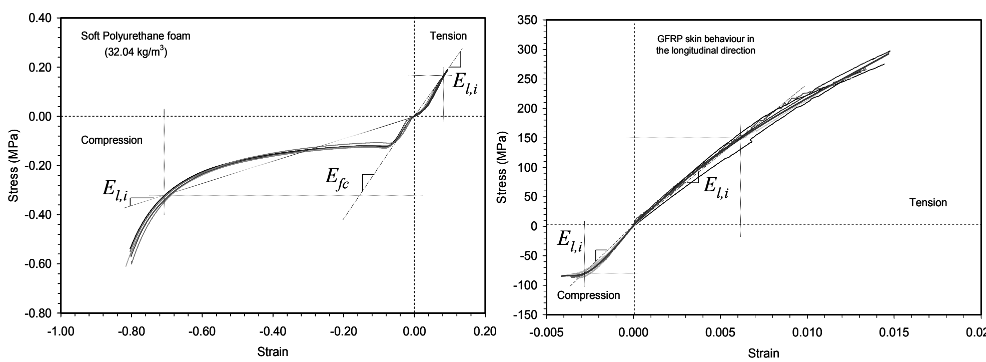

At any segment l and for any layer i

$$\text{Transformed width, } b_{t,l,i} = b_{l,i}\,\frac{E_{l,i}}{E_{fc}}$$

Figure 8. Section transformation accounting for variable modulus in core and skin in tension and compression

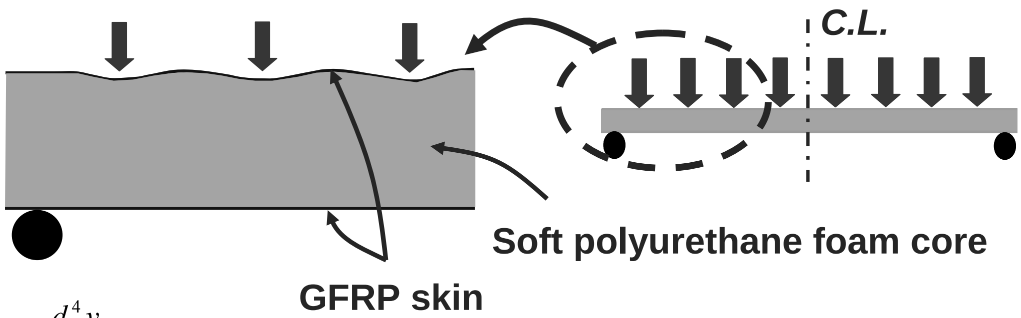

$$EI\frac{d^4y}{dx^4}+ky=0$$

$$y=e^{\beta x}\left(C_1\cos\beta x \quad + \quad C_2\sin\beta x\right) \quad + \quad e^{-\beta x}\left(C_3\cos\beta x \quad + \quad C_4\sin\beta x\right)$$

$$\beta=\sqrt[4]{\frac{k}{4EI}}$$

Flexural Defl. Shear Defl.

Winkler Defl.

<u>**Total Midspan Deflection of Top Skin.**</u>

$$\delta_{total}=\delta_m+\delta_v+\delta_w$$

<u>**New sec. Height**</u>

$$H_{new,l}=H_{old,l}-\left|\delta_{v,top,l}-\delta_{v,bot,l}\right|-\delta_{w,l}$$

Figure 9. Winkler effect of polyurethane foam softness at loading points

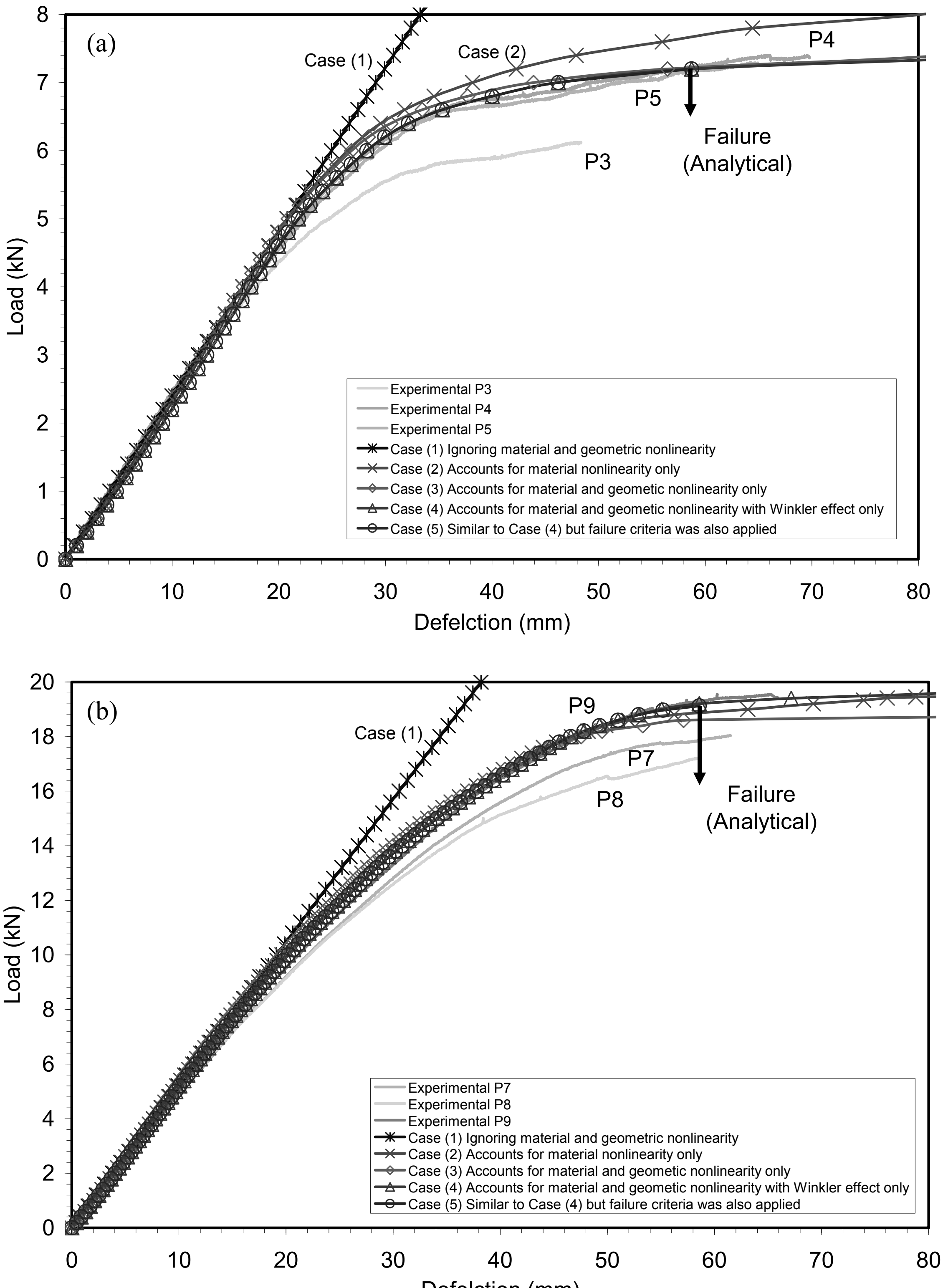

Figure 10. Illustration of significance of various features of the model for sandwich panels: (a) with soft cores, Specimen P3 to P5; and (b) with hard cores, Specimen P7 to P9; tested by Shawkat (2008)

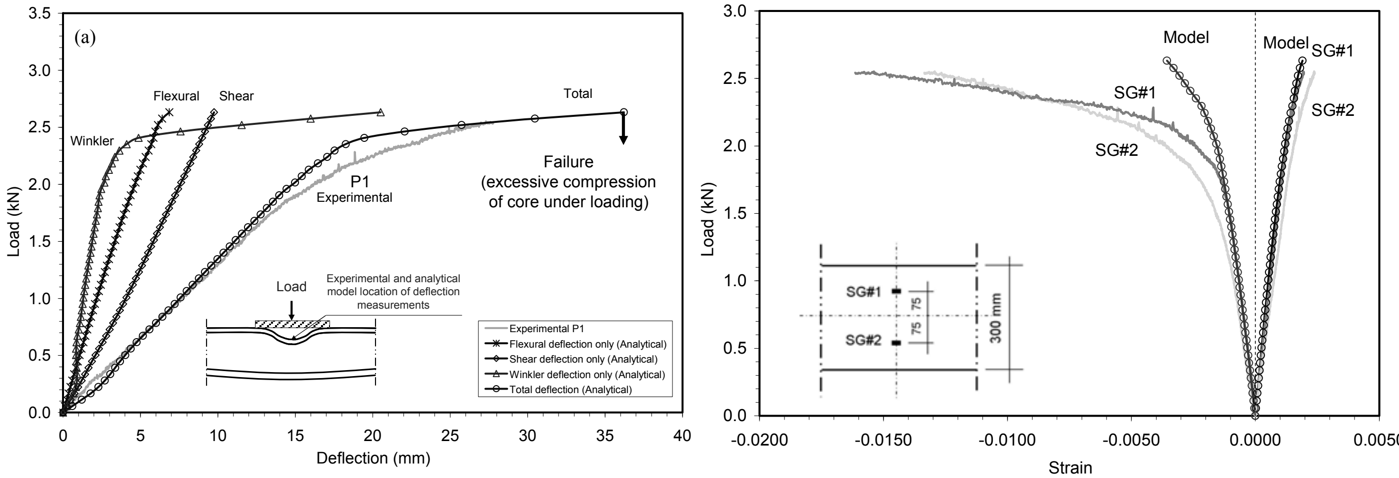

(a) Panel P1 tested under a concentrated load in three-point bending

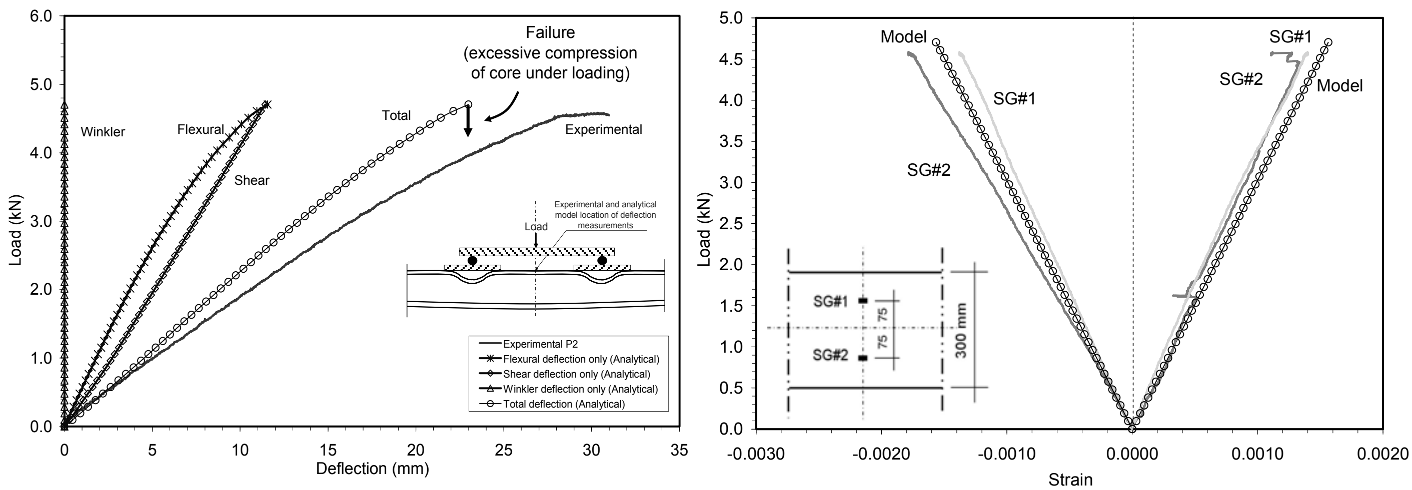

(b) Panel P2 tested under two concentrated loads in four-point bending

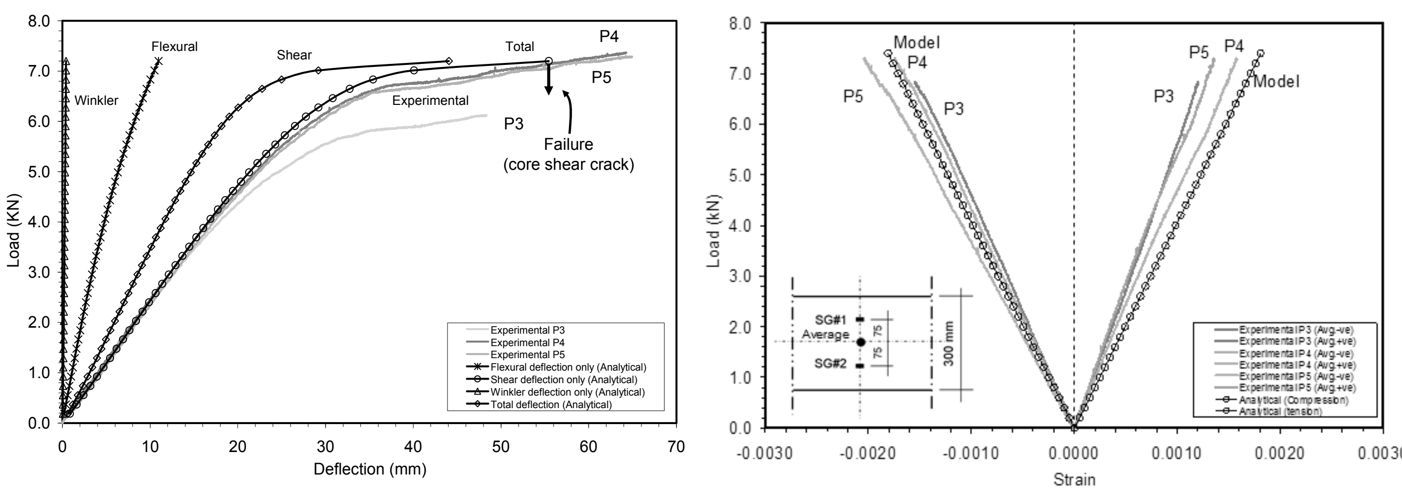

(c) Panels P3-P5 tested under uniformly distributed load

Figure 11. Model verification using load-deflection and load-longitudinal strain responses of panels with low density cores tested by Shawkat (2008)

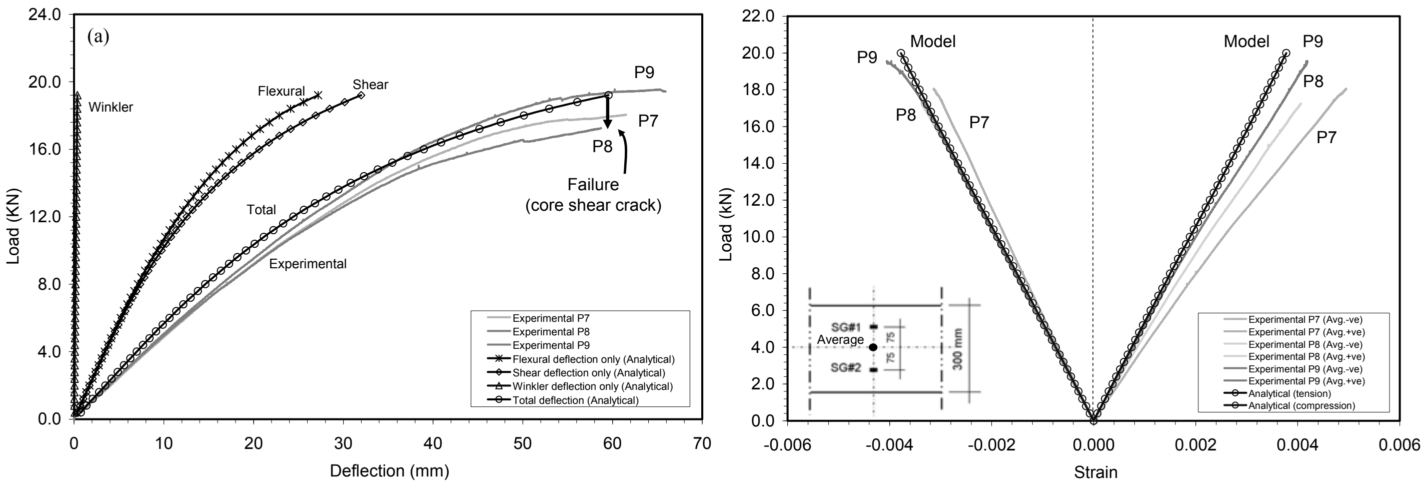

Figure 12. Model verification using load-deflection and load-longitudinal strain responses of panels P7-P9 with high density cores tested by Shawkat (2008) under uniformly distributed load

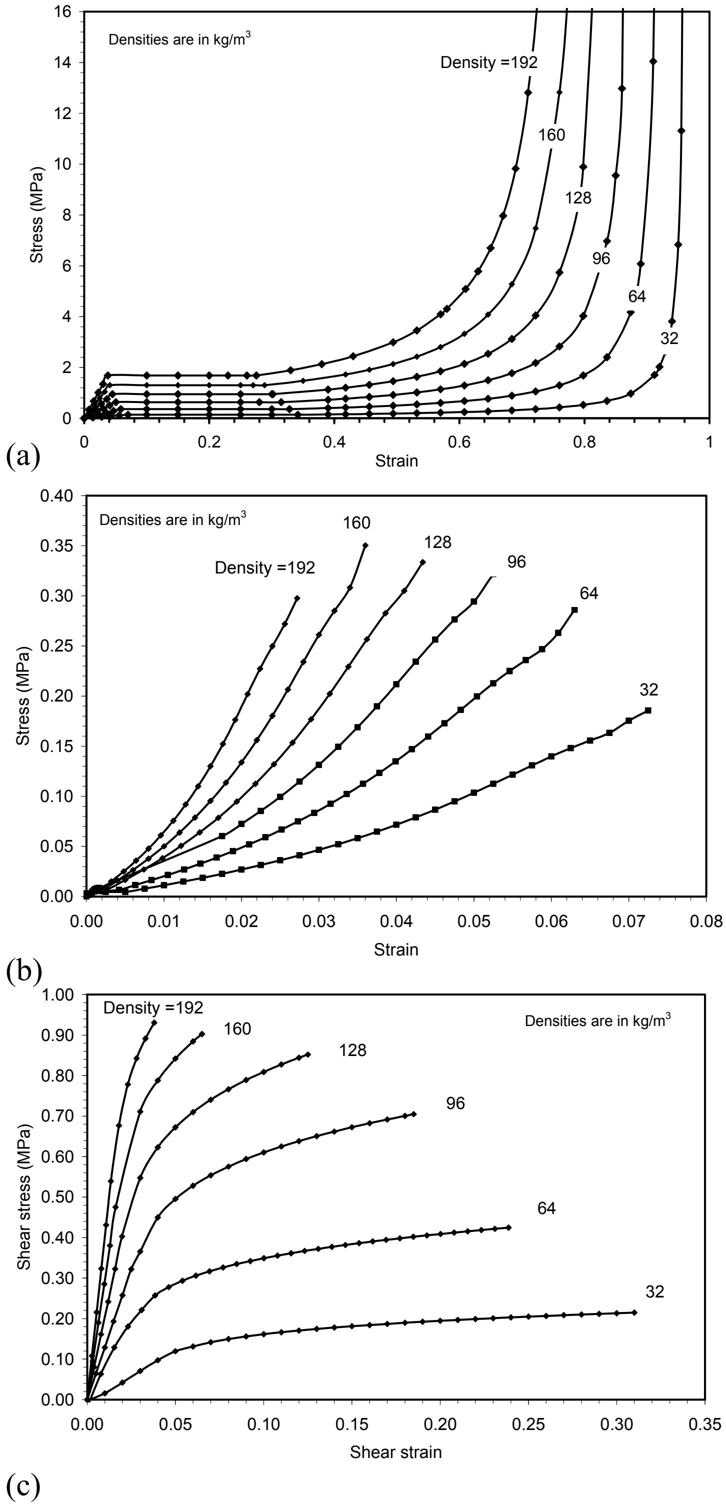

Figure 13. Stress-strain curves for polyurethane foam with densities ranging from 32 kg/m3 to 192 kg/m^3: (a) in compression, (b) in tension and (c) in shear

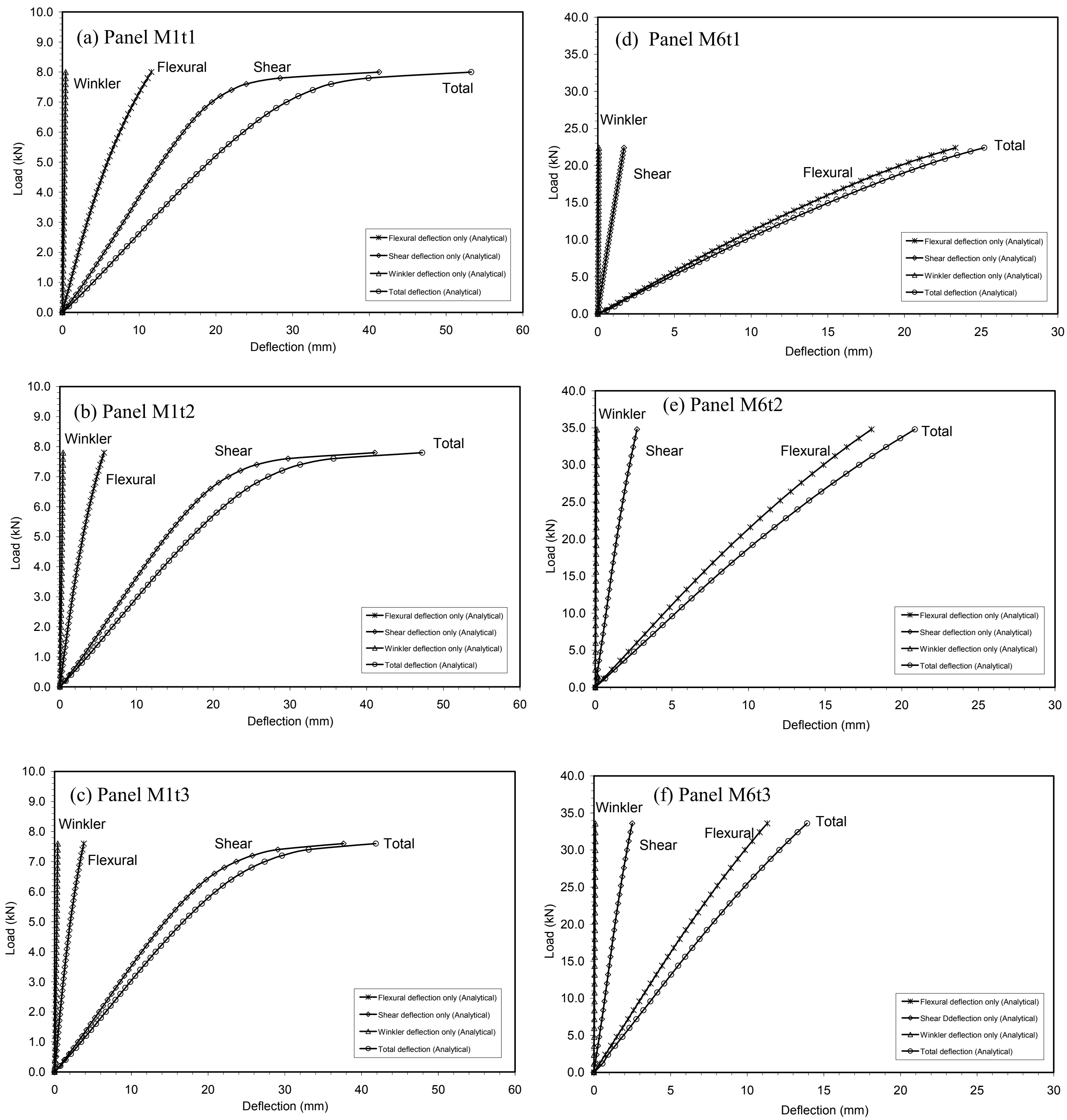

Figure 14. Effect of core density and skin thickness on load-deflection responses of panels.

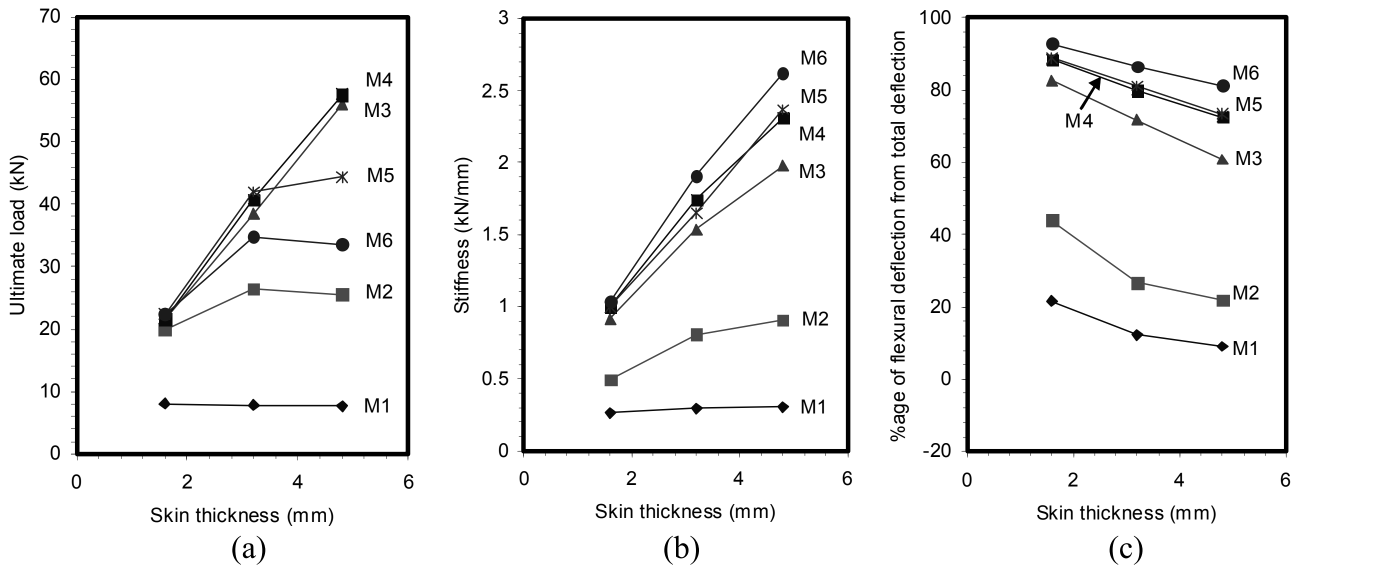

Figure 15. Effect of skin thickness on behaviour of panels with different core densities: (a) ultimate load, (b) stiffness, and (c) percentage of flexural deflection to total deflection

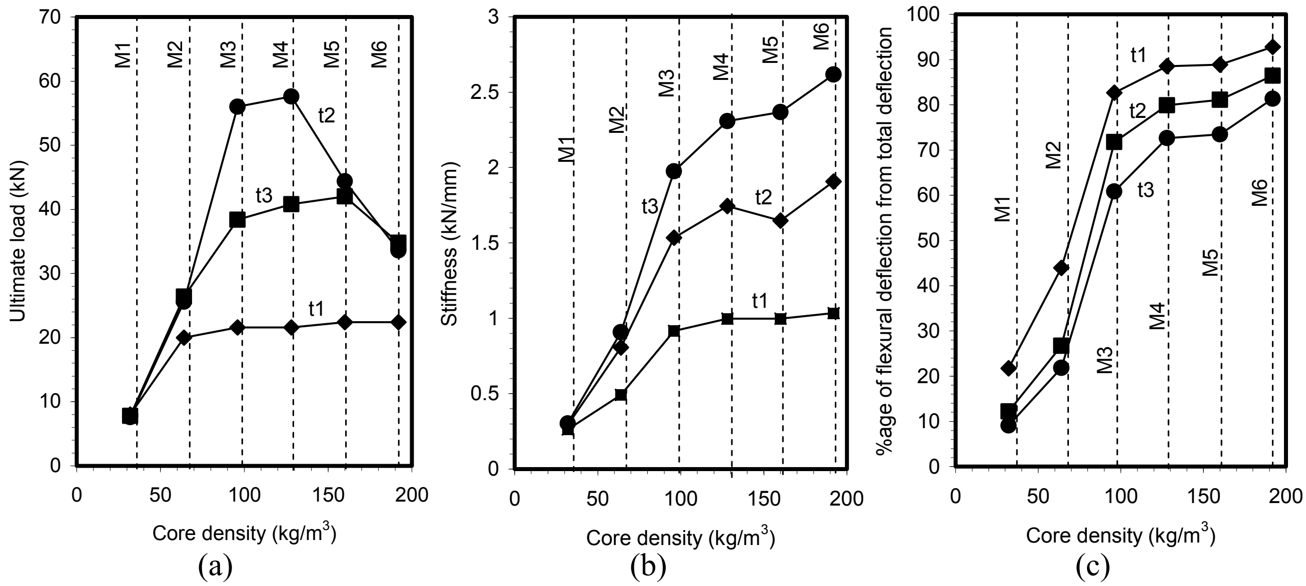

Figure 16. Effect of core density on behaviour of panels with different skin thicknesses: (a) ultimate load, (b) stiffness, and (c) percentage of flexural deflection to total deflection